JACS
JOURNAL OF THE AMERICAN CHEMICAL SOCIETY

Communication

pubs.acs.org/JACS

Single-Molecule Spectroscopy of Cold Denaturation and the Temperature-Induced Collapse of Unfolded Proteins

Mikayel Aznauryan, Daniel Nettels, Andrea Holla, Hagen Hofmann, and Benjamin Schuler*

Department of Biochemistry, University of Zurich, Winterthurerstrasse 190, 8057 Zurich, Switzerland

Supporting Information

ABSTRACT: Recent Förster resonance energy transfer (FRET) experiments show that heat-unfolded states of proteins become more compact with increasing temperature. At the same time, NMR results indicate that cold-denatured proteins are more expanded than heat-denatured proteins. To clarify the connection between these observations, we investigated the unfolded state of yeast frataxin, whose cold denaturation occurs at temperatures above 273 K, with single-molecule FRET. This method allows the unfolded state dimensions to be probed not only in the cold- and heat-denatured range but also in between, i.e., in the presence of folded protein, and can thus be used to link the two regimes directly. The results show a continuous compaction of unfolded frataxin from 274 to 320 K, with a slight re-expansion at higher temperatures. Cold- and heat-denatured states are thus essentially two sides of the same coin, and their behavior can be understood within the framework of the overall temperature dependence of the unfolded state dimensions.

Proteins can unfold not only at high but also low temperatures, a behavior that has been quantified thoroughly in terms of the underlying thermodynamics of protein stability.[1] The molecular details of cold denaturation are still under debate, but the most common interpretation of the origin of this phenomenon is the decreasing strength of the hydrophobic effect with decreasing temperature, which is expected to be connected to changes in the structure and dynamics of the hydration layer around the polypeptide chain.[2−6] However, a detailed structural investigation of cold denaturation and possible differences in the structure of cold- and heat-denatured proteins has only become possible rather recently, with the discovery of proteins for which the cold-denatured state is populated above the melting point of water and is thus experimentally accessible without the addition of denaturants.[7−10] Based on NMR experiments, differences in residual secondary structure and the degree of protein hydration in cold- and heat-denatured states have been identified.[11−13] Another remarkable observation, based on NMR measurements on the C-terminal domain of protein L9 in the cold-denatured state, was a trend of increasing radii of hydration as the temperature was reduced.[7,9] This result suggests an interesting possible connection to recent single-molecule and ensemble Förster resonance energy transfer (FRET) experiments that demonstrated a continuous compaction of chemically, heat-, and pH-unfolded proteins with increasing temperature.[14,15] These possibly counterintuitive observations indicate the presence of interactions within the unfolded polypeptide chain that increase with temperature. However, the quantitative link between the NMR and the FRET experiments has remained unclear, especially whether the dimensions of the unfolded state populated upon cold denaturation deviate from the trend observed upon heat denaturation.[16]

Here, we address this question by investigating the temperature dependence of the cold- and heat-denatured states of yeast frataxin (Yfh1), which was chosen specifically as one of the very few available systems that would allow us to probe the properties of the unfolded state both under conditions of complete heat and almost complete cold denaturation (and in between) without extrapolation from high denaturant concentrations or extremes of pH. Even at the temperature of maximum conformational stability, a fraction of the population remains unfolded, which is an essential prerequisite for us to monitor the denatured state over the entire temperature range, from 274 to 332 K, and thus to directly link the behavior of cold- and heat-denatured protein. To probe the dimensions of unfolded frataxin, we use single-molecule FRET, which has been employed for measurements of intramolecular distances and distance distributions for a wide range of proteins denatured by chaotropes and heat, and for intrinsically disordered proteins.[14,17−25] As a key advantage, single-molecule FRET allows a clear separation of folded and unfolded subpopulations, and thus a quantitative analysis of the properties of the unfolded state without influence of the folded state signal, which is often difficult to achieve in ensemble experiments.[26]

For the single-molecule experiments, we created a double cysteine variant (C47S, N16C, S120C) of Yhf1. To quantify the effect of the Cys mutations on the conformational stability of Yhf1, circular dichroism (CD) experiments on the unlabeled protein were performed (Figure 1). The negative ellipticity is maximal at 289 K, corresponding to the temperature of highest conformational stability. The decreasing secondary structure content below and above 289 K correspond to cold and heat denaturation, respectively, as illustrated by the fraction of folded protein, $F_f(T)$, as a function of temperature T (Figure 1C). The data were fitted with $F_f(T) = (1 - \exp(-\Delta G_U/RT))^{-1}$, where the free energy of unfolding, $\Delta G_U(T)$, is parametrized in terms of T_S, the temperature where $\Delta G_U(T)$ is maximal; ΔH_S, the unfolding enthalpy at that temperature; and

Received: July 9, 2013
Published: September 8, 2013

   dx.doi.org/10.1021/ja407009w | J. Am. Chem. Soc. 2013, 135, 14040−14043

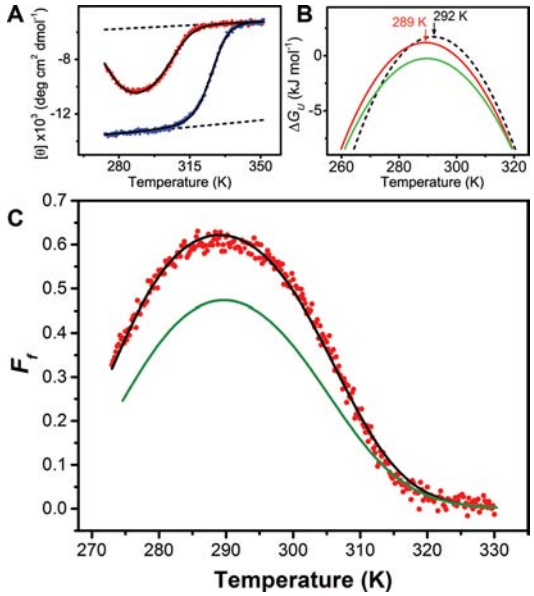

Figure 1. (A) Temperature dependence of the conformational stability of Yfh1 monitored by changes in ellipticity at 222 nm (red dots). The baseline for the unfolded subpopulation (upper dashed line) was obtained by linear extrapolation of the high temperature data. For obtaining a baseline for the folded subpopulation (lower dashed line), the protein was stabilized by adding 0.3 M sodium sulfate (blue dots). The black solid lines show fits with ΔH_S, ΔC_p, and T_S as fit parameters (see SI for details). (B) Temperature dependences of the unfolding free energy, ΔG_U, for the double-Cys variant of Yhf1 based on the thermodynamic parameters derived from CD (red line) and for the labeled protein as derived from single-molecule FRET (green line, Figure 2). The dashed black line represents the stability curve obtained by Pastore et al. for wild-type Yhf1 in 20 mM HEPES buffer.[8] (C) Temperature dependence of the fraction of folded (F_f) Yfh1 (red dots) as obtained from the data in (A), with a fit using eqs S14 and S15 (SI) shown as a solid line. The fit from Figure 3A is shown as a green line for direct comparison with the FRET results.

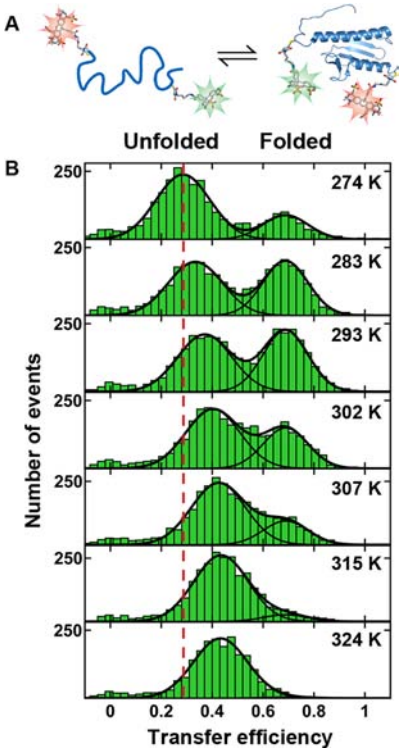

Figure 2. (A) Cartoons of unfolded and folded Yfh1 (based on PDB ID 2GA5) with Alexa Fluor 488 (green) and Alexa Fluor 594 (red) dyes at positions N16C and S120C. (B) Representative examples of single-molecule FRET efficiency histograms of Yfh1 show heat and cold denaturation and a temperature-induced collapse of the unfolded protein. The peak at E = 0.7 corresponds to folded and the peak at lower transfer efficiency to unfolded molecules. To determine mean transfer efficiencies, peaks were fit with Gaussian distributions (black lines); the width of the unfolded-state peak and the position and width of the folded-state peak were used as global fit parameters and are thus identical for all histograms. The red dashed line indicates the position of the unfolded peak at 274 K.

ΔC_p, the change in heat capacity upon unfolding (see SI for details). The $\Delta G_U(T)$ dependence calculated from the resulting thermodynamic parameters is close to the dependence found by Pastore et al.[8,27] for wild-type Yhf1 (Figure 1B, Table S1).

The protein was then labeled with Alexa Fluor 488 and Alexa Fluor 594 as FRET donor and acceptor, respectively (Figure 2A). Confocal single-molecule fluorescence spectroscopy on molecules freely diffusing in solution was used to quantify the equilibrium between folded and unfolded states and to separate the corresponding subpopulations. Bursts of fluorescence photons, detected while single frataxin molecules diffused through the laser focus of the confocal instrument, were used to obtain transfer efficiency histograms between 274 and 332 K. Examples are shown in Figure 2B. To eliminate the contribution from the molecules lacking an active acceptor at a transfer efficiency of $E \approx 0$, we used pulsed interleaved excitation[28] (see SI for details). We observe two peaks, as expected for cooperative cold- and heat-unfolding transitions that can be well approximated by a two-state process.[9] The peak at a transfer efficiency of E = 0.7 corresponds to the subpopulation of folded proteins. The peak centered at transfer efficiencies between E = 0.23 and E = 0.43 corresponds to the subpopulation of unfolded protein. The transfer efficiency histograms illustrate directly that the unfolded state is present over the entire temperature range, while the relative populations of folded and unfolded subpopulations vary.

From the transfer efficiency histograms, the fractions of folded protein molecules are obtained from the relative peak areas. The resulting temperature dependence (Figure 3A) shows that the folded state is maximally populated at about 290 K. Both with decreasing and increasing temperature, we observe the decrease in folded population and concomitant increase in the unfolded population expected for cold and heat denaturation. The good agreement of the corresponding stability curve with the results from unlabeled protein (Figure 1B,C) indicates that the thermodynamic properties of the sample are only marginally affected by FRET labeling.

The separation of native and unfolded subpopulations in the single-molecule experiments allows us to investigate not only the effect of temperature on the equilibrium between the two thermodynamic states, but, more importantly, it allows us to quantify changes in transfer efficiency for the unfolded subpopulation over the entire temperature range, even in the presence of folded molecules. The change in mean transfer efficiency of the unfolded state with temperature is apparent in Figure 2, indicating a change in the average distance between the fluorophores. To analyze the single-molecule data in terms of the dimensions of the unfolded state, we converted the mean transfer efficiencies obtained from the corresponding peaks to

dx.doi.org/10.1021/ja407009w | J. Am. Chem. Soc. 2013, 135, 14040−14043

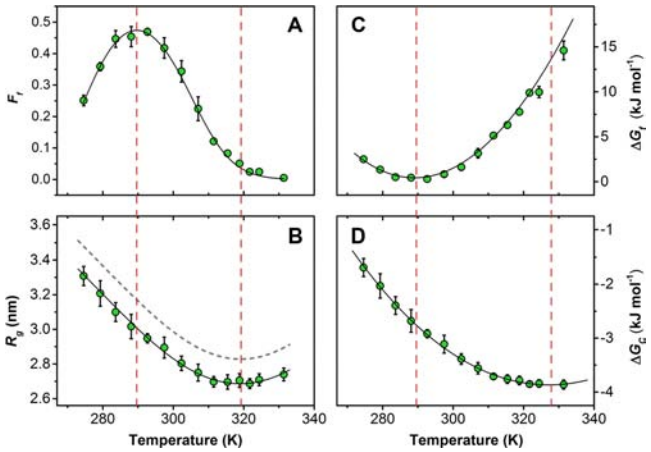

Figure 3. (A) Relative fraction of folded Yhf1 (F_f) calculated as a ratio of the area of the "folded" peak and the sum of the areas of "folded" and "unfolded" peaks with a fit as in Figure 1C (black line). (B) Temperature dependence of the measured radius of gyration (R_g) of unfolded Yfh1 (circles). The R_g values correspond to the interdye segment of the protein chain including the two dye linkers (each estimated to be equivalent to 4.5 peptide bonds[21]). The solid line represents a fit of R_g as a function of temperature (see details in SI). For comparison, we also show the fit of the radii of gyration rescaled to the full-length sequence (gray dashed line, see SI). (C) Temperature dependence of the free energy of folding (ΔG_f) of labeled Yhf1 calculated from the data in (A). (D) Temperature dependence of the free energy of collapse (ΔG_C) of unfolded Yhf1, calculated with respect to the excluded volume limit, where $\varepsilon = 0$ (see SI). Black solid lines in (C) and (D) are fits to the data assuming a constant heat capacity. Error bars indicate standard deviations estimated from three independent measurements.

mean radii of gyration based on polymer physical distance distributions[14,19,21,23,24,29] (see SI for details). Here we use the coil-to-globule transition theory of Sanchez,[19,24,29,30] but the results are robust with respect to the details of the shape of the distance distribution used (Figure S4).

Figure 3B shows the resulting values of the radius of gyration, R_g, of the denatured state as a function of temperature over a broad range, bridging the regimes of cold and heat denaturation. These data show a decrease of R_g of the unfolded state of Yhf1 from 273 to ∼320 K, corresponding to a continuous collapse of the unfolded chain with increasing temperature, followed by a slight re-expansion at temperatures above 320 K (Figure 3B). The temperature regime above 335 K is currently not accessible experimentally because of a rapid loss of signal, presumably due to accelerated photodestruction of the fluorophores. For a quantitative comparison of the intramolecular energetics relevant for folding and unfolded state collapse, respectively, the protein stability curve, $\Delta G_f(T)$, and the free energy of collapse, $\Delta G_C(T)$, as obtained from Sanchez theory (see SI for details), are also shown in Figure 3C,D.

The temperature dependence of R_g observed here for the denatured state illustrates an important point: the expansion of the cold-denatured state with decreasing temperature, as observed in NMR experiments,[7,9] and the collapse of unfolded proteins with increasing temperature detected by single-molecule spectroscopy[14] are essentially two sides of the same coin—an overall continuous change in denatured state dimensions with temperature. This observation is in line with the notion of the thermodynamic equivalence of cold- and heat-denatured states,[1] but at the same time demonstrates the non-cooperative shift of the distance distribution in the unfolded state with temperature. This conclusion is further corroborated by experiments with a second variant of frataxin with the FRET dyes in positions that allow us to investigate the unfolded state dimensions without overlap with the folded-state peak, which shows the same behavior (Figure S5). The similarity to the temperature dependence of heat-unfolded CspTm[16] suggests that what we observe is a rather generic behavior of denatured states, independent of whether they are populated by heating or cooling.

An interesting observation is the non-monotonic dependence of the R_g of unfolded frataxin on temperature. Remarkably, such behavior with a minimum in $R_g(T)$ has been observed even in simulations of hydrophobic homopolymers[3,31−34] and simple heteropolymers[35] in explicit water. In such simulations, the most compact ensemble has typically been assumed to resemble the folded state of a protein, and the expansions at low and high temperatures have been taken to correspond to cold and heat unfolding, respectively. In contrast, our results illustrate that the overall energetics of protein folding on the one hand and unfolded state collapse on the other are quite different (Figure 3): while $\Delta G_f(T)$ has a minimum at ∼290 K, where the native state of frataxin is most stable, the free energy of collapse, $\Delta G_C(T)$, has a minimum at ∼328 K, where the denatured state is most compact. However, $\Delta G_f(T)$ and $\Delta G_C(T)$ share the non-monotonic temperature dependence usually taken as an indication for the involvement of hydrophobic hydration.[2,36] Given the absence of specific interactions in simple polymer models,[3,31−35] the compact state observed in corresponding simulations is thus likely to resemble the compact unfolded state observed here rather than a folded state.

Recent NMR chemical shift experiments confirm the importance of hydration for the properties of the unfolded state and indicate pronounced differences in the degree of hydrogen bonding of backbone amides with water in cold- and heat-denatured yeast frataxin,[13] a process that is probably closely linked to slight changes in secondary structure content,[13] as previously suggested for other unfolded proteins.[14,37] Similarly, molecular dynamics simulations of the temperature dependence of unfolded state dimensions are very sensitive to the water model used, indicating a crucial role of hydration.[23] Both polymer expansion at low temperature and cold denaturation have been rationalized in terms of effects that favor the formation of a hydrated denatured form over a compact state at low temperature. Mechanistic explanations include a reduced probability of cavity formation in the solvent required for local dewetting and concomitant formation of a hydrophobic core;[38] lower hydrogen bond energy for hydration shell water compared to bulk water at low temperature;[3] or, closely connected, a reduction in water entropy at low temperature.[39]

But why is the minimum of $\Delta G_f(T)$ shifted by almost 40 K relative to $\Delta G_C(T)$? $\Delta G_f(T)$ consists of at least three contributions: the difference in internal energy of folded and unfolded states, ΔU_f; the difference in solvation free energy of folded and unfolded states, ΔG_s; and a term due to the difference in configurational entropy of folded and unfolded states,[40] $T\Delta S_{conf}$. ΔU_f may be expected to exhibit little temperature dependence, but we expect a strong effect of $T\Delta S_{conf}$ on the position of the minimum of $\Delta G_f(T)$, since $|\Delta S_{conf}|$ is much larger for folding than for unfolded state

dx.doi.org/10.1021/ja407009w | J. Am. Chem. Soc. 2013, 135, 14040−14043

collapse. Additional contributions to the difference between $\Delta G_f(T)$ and $\Delta G_C(T)$ may come from the change in the temperature dependence of the excess chemical potential of cavity formation in water with the size of the solute in the crossover region of ∼1 nm, as suggested by theory and simulation:[41] the less specific and transiently formed hydrophobic clusters present in a denatured protein are expected to be relatively small, and their hydration may thus exhibit a temperature dependence different from the formation of the folded state, which is larger and has a different surface composition. The recent emergence of force fields and water models that provide a more realistic description of unfolded and disordered proteins[42,43] may allow a more detailed identification of the molecular processes underlying cold denaturation, whose close interrelation with the continuous temperature-induced unfolded-state collapse is demonstrated here. In summary, our work thus connects previously disconnected observations on the unfolded state populated either through cold or heat denaturation by understanding its behavior within the framework of the temperature-dependent dimensions of a single denatured state.

■ ASSOCIATED CONTENT

Supporting Information

Experimental procedures, data analysis, and single-molecule data for a second variant of frataxin. This material is available free of charge via the Internet at http://pubs.acs.org.

■ AUTHOR INFORMATION

Corresponding Author

schuler@bioc.uzh.ch

Notes

The authors declare no competing financial interest.

■ ACKNOWLEDGMENTS

We thank Robert Best and Jeetain Mittal for discussions regarding hydrophobic hydration and conformational entropy, and Andrea Soranno for help with data analysis. This work was supported by the Swiss National Science Foundation and by the Forschungskredit of the University of Zurich.

■ REFERENCES

(1) Privalov, P. L. *Crit. Rev. Biochem. Mol. Biol.* **1990**, *25*, 281.
(2) Privalov, P. L.; Gill, S. J. *Adv. Protein Chem.* **1988**, *39*, 191.
(3) Dias, C. L.; Ala-Nissila, T.; Karttunen, M.; Vattulainen, I.; Grant, M. *Phys. Rev. Lett.* **2008**, *100*, No. 118101.
(4) Yoshidome, T.; Kinoshita, M. *Phys. Rev. E* **2009**, *79*, No. 030905(R).
(5) Graziano, G. *Phys. Chem. Chem. Phys.* **2010**, *12*, 14245.
(6) Dias, C. L. *Phys. Rev. Lett.* **2012**, *109*, No. 048104.
(7) Li, Y.; Shan, B.; Raleigh, D. P. *J. Mol. Biol.* **2007**, *368*, 256.
(8) Pastore, A.; Martin, S. R.; Politou, A.; Kondapalli, K. C.; Stemmler, T.; Temussi, P. A. *J. Am. Chem. Soc.* **2007**, *129*, 5374.
(9) Luan, B.; Shan, B.; Baiz, C.; Tokmakoff, A.; Raleigh, D. P. *Biochemistry* **2013**, *52*, 2402.
(10) Buchner, G. S.; Shih, N.; Reece, A. E.; Niebling, S.; Kubelka, J. *Biochemistry* **2012**, *51*, 6496.
(11) Adrover, M.; Esposito, V.; Martorell, G.; Pastore, A.; Temussi, P. A. *J. Am. Chem. Soc.* **2010**, *132*, 16240.
(12) Shan, B.; McClendon, S.; Rospigliosi, C.; Eliezer, D.; Raleigh, D. P. *J. Am. Chem. Soc.* **2010**, *132*, 4669.
(13) Adrover, M.; Martorell, G.; Martin, S. R.; Urosev, D.; Konarev, P. V.; Svergun, D. I.; Daura, X.; Temussi, P.; Pastore, A. *J. Mol. Biol.* **2012**, *417*, 413.
(14) Nettels, D.; Muller-Spath, S.; Kuster, F.; Hofmann, H.; Haenni, D.; Ruegger, S.; Reymond, L.; Hoffmann, A.; Kubelka, J.; Heinz, B.; Gast, K.; Best, R. B.; Schuler, B. *Proc. Natl. Acad. Sci. U.S.A.* **2009**, *106*, 20740.
(15) Sadqi, M.; Lapidus, L. J.; Munoz, V. *Proc. Natl. Acad. Sci. U.S.A.* **2003**, *100*, 12117.
(16) Nettels, D.; Müller-Späth, S.; Küster, F.; Hofmann, H.; Haenni, D.; Rüegger, S.; Reymond, L.; Hoffmann, A.; Kubelka, J.; Heinz, B.; Gast, K.; Best, R. B.; Schuler, B. *Proc. Natl. Acad. Sci. U.S.A.* **2009**, *106*, 20740.
(17) Deniz, A. A.; Laurence, T. A.; Beligere, G. S.; Dahan, M.; Martin, A. B.; Chemla, D. S.; Dawson, P. E.; Schultz, P. G.; Weiss, S. *Proc. Natl. Acad. Sci. U.S.A.* **2000**, *97*, 5179.
(18) Schuler, B.; Lipman, E. A.; Eaton, W. A. *Nature* **2002**, *419*, 743.
(19) Sherman, E.; Haran, G. *Proc. Natl. Acad. Sci. U.S.A.* **2006**, *103*, 11539.
(20) Michalet, X.; Weiss, S.; Jager, M. *Chem. Rev.* **2006**, *106*, 1785.
(21) Hoffmann, A.; Kane, A.; Nettels, D.; Hertzog, D. E.; Baumgartel, P.; Lengefeld, J.; Reichardt, G.; Horsley, D. A.; Seckler, R.; Bakajin, O.; Schuler, B. *Proc. Natl. Acad. Sci. U.S.A.* **2007**, *104*, 105.
(22) Merchant, K. A.; Best, R. B.; Louis, J. M.; Gopich, I. V.; Eaton, W. A. *Proc. Natl. Acad. Sci. U.S.A.* **2007**, *104*, 1528.
(23) Muller-Spath, S.; Soranno, A.; Hirschfeld, V.; Hofmann, H.; Ruegger, S.; Reymond, L.; Nettels, D.; Schuler, B. *Proc. Natl. Acad. Sci. U.S.A.* **2010**, *107*, 14609.
(24) Hofmann, H.; Soranno, A.; Borgia, A.; Gast, K.; Nettels, D.; Schuler, B. *Proc. Natl. Acad. Sci. U.S.A.* **2012**, *109*, 16155.
(25) Soranno, A.; Buchli, B.; Nettels, D.; Cheng, R. R.; Muller-Spath, S.; Pfeil, S. H.; Hoffmann, A.; Lipman, E. A.; Makarov, D. E.; Schuler, B. *Proc. Natl. Acad. Sci. U.S.A.* **2012**, *109*, 17800.
(26) Schuler, B.; Eaton, W. A. *Curr. Opin. Struct. Biol.* **2008**, *18*, 16.
(27) Martin, S. R.; Esposito, V.; Rios, P. D. L.; Pastore, A.; Temussi, P. A. *J. Am. Chem. Soc.* **2008**, *130*, 9963.
(28) Muller, B. K.; Zaychikov, E.; Brauchle, C.; Lamb, D. C. *Biophys. J.* **2005**, *89*, 3508.
(29) Ziv, G.; Haran, G. *J. Am. Chem. Soc.* **2009**, *131*, 2942.
(30) Sanchez, I. C. *Macromolecules* **1979**, *12*, 980.
(31) Paschek, D.; Nonn, S.; Geiger, A. *Phys. Chem. Chem. Phys.* **2005**, *7*, 2780.
(32) De los Rios, P.; Caldarelli, G. *Phys. Rev. E* **2001**, *63*, No. 031802.
(33) Das, P.; Matysiak, S. *J. Phys. Chem. B* **2012**, *116*, 5342.
(34) Matysiak, S.; Debenedetti, P. G.; Rossky, P. J. *J. Phys. Chem. B* **2012**, *116*, 8095.
(35) Jamadagni, S. N.; Bosoy, C.; Garde, S. *J. Phys. Chem. B* **2010**, *114*, 13282.
(36) Southall, N. T.; Dill, K. A.; Haymet, A. D. J. *J. Phys. Chem. B* **2002**, *106*, 521.
(37) Yang, W. Y.; Larios, E.; Gruebele, M. *J. Am. Chem. Soc.* **2003**, *125*, 16220.
(38) ten Wolde, P. R.; Chandler, D. *Proc. Natl. Acad. Sci. U.S.A.* **2002**, *99*, 6539.
(39) Oshima, H.; Yoshidome, T.; Amano, K.; Kinoshita, M. *J. Chem. Phys.* **2009**, *131*, No. 205102.
(40) Thompson, J. B.; Hansma, H. G.; Hansma, P. K.; Plaxco, K. W. *J. Mol. Biol.* **2002**, *322*, 645.
(41) Lum, K.; Chandler, D.; Weeks, J. D. *J. Phys. Chem. B* **1999**, *103*, 4570.
(42) Best, R. B.; Mittal, J. *J. Phys. Chem. B* **2010**, *114*, 14916.
(43) Best, R. B.; Hummer, G. *J. Phys. Chem. B* **2009**, *113*, 9004.